Available online at www.sciencedirect.com
ScienceDirect
Trans. Nonferrous Met. Soc. China 23(2013) 2857−2862
Transactions of Nonferrous Metals Society of China
www.tnmsc.cn

High temperature tensile deformation behavior of AZ80 magnesium alloy

Jun QIAO, Fu-bo BIAN, Min HE, Yu WANG

School of Materials Science and Metallurgy, University of Science and Technology Liaoning, Anshan 114051, China

Received 9 September 2012; accepted 13 March 2013

Abstract: Tensile behaviors of an AZ80 alloy were investigated by elongation-to-failure tensile tests at 300, 350, 400 and 450 °C, and strain rates of 10^{-2} and 10^{-3} s^{-1}. Strain-rate-change tests from 5×10^{-5} s^{-1} to 2×10^{-2} s^{-1} were applied to study deformation mechanisms. The experimental data show that the material exhibits enhanced tensile ductilities of over 100% at 400 and 450 °C with stress exponent of 4.29 and activation energy of 149.60 kJ/mol, and initial fine grains preserve in evenly deformed gauge based on microstructure studies. The enhanced tensile ductilities are rate controlled by a competitive mechanism of grain boundary sliding and dislocation climb creep, based on which a model can successfully simulate the deformation behavior.

Key words: AZ80 magnesium alloy; tensile behavior; superplasticity; creep; stress exponent

1 Introduction

Magnesium (Mg) alloys have attracted significant interests as a mass-saving replacement for steel and aluminum alloys in vehicles and electronic products due to their low density, high specific strength, and excellent shock resistance [1,2]. To date, applications of Mg alloy sheets have been greatly limited because of their low room-temperature formability inheriting from the hexagonally close-packed crystal structure with only two active and independent base slip systems. Fortunately, prismatic and pyramidal slip systems activated at high temperatures do facilitate dislocation creep, which is critical to ductility enhancement of Mg alloys with less-refined grains, and to superplastic production of complex components that cannot be economically formed at room temperature.

Enhanced high temperature ductility of Mg alloys can be achieved by mechanisms of grain boundary sliding (GBS), solute-drag creep (SDC), and dislocation climb creep (DCC). These mechanisms are generally described by the constitutive equation for crystalline materials [3]:

$$\dot{\varepsilon}=\frac{ADGb}{kT}\left(\frac{b}{d}\right)^{p}\left(\frac{\sigma}{G}\right)^{n} \tag{1}$$

$$D=D_0\exp(-Q/RT) \tag{2}$$

where $\dot{\varepsilon}$ is the creep rate; A is a constant related to the material; D is the appropriate diffusivity; D_0 is the preexponential factor; Q is the activation energy; R is the gas constant; G is the shear modulus; b is the Burgers vector; k is the Boltzmann constant; T is the absolute temperature in K; d is the grain size; is the flow stress; p is the grain size exponent and n is the stress exponent.

GBS with a typical stress exponent of $n\approx2$ operates as a major mechanism of fine-grained superplasticity by grain boundary or intracrystalline diffusion at low stress and high temperature. GBS requires a fine and stable grain size of the order of 10 μm, which is specially realized by high cost metallurgical and processing techniques such as powder metallurgy, rapid solidification, and equal channel angular pressing [4−8]. However, the contribution of GBS to total plastic strain decreases with increasing stress or strain rate, since intracrystalline dislocations become more active and DCC dominates deformation with $n\geq5$. DCC is controlled by dislocation climb rate which is related to vacancy diffusion, and the activation energy is about equal to that of lattice self diffusion [9,10]. Dislocation slide and climb operate sequentially, and the slower one determines dislocation velocity and strain rate. Therefore, SDC may dominate deformation if dislocation glide is

Foundation item: Project (50801034) supported by the National Natural Science Foundation of China; Project (LJQ 2011026) supported by Development Foundation for Excellent Young Scholars in Universities of Liaoning Province, China; Project (2006207) supported by Foundation for "Ten-Hundred-Thousand" High-end Talent Introduction Project in Liaoning Province, China

Corresponding author: Jun QIAO; Tel: +86-412-5929532; E-mail: qiaojun@ustl.edu.cn

DOI: 10.1016/S1003-6326(13)62807-1

interacted and retarded by a dragging force of solute atoms. This elastic interaction between stress field of sliding dislocation and solute atoms causes viscous glide of dislocations, and typically presents a stress exponent of $n \approx 3$ and activation energy for solute atom chemical diffusion [11]. SDC is not sensitive to grain size, p=0, and is important to improve ductility of Mg alloys with relatively coarse grains.

AZ80 alloy with high Al content of ~8% (mass fraction) offers higher strength, lower formability, and higher operation possibility of SDC than AZ31. However, high temperature deformation behaviors and mechanisms related to GBS, SDC, and DCC have not been thoroughly studied for AZ80 alloy. This work is to investigate these features through high temperature tensile tests, microstructure observations, and mechanism analyses.

2 Experimental

An AZ80 slab of 12 mm thickness was extruded from a round billet of ϕ165 mm, and then was reduced to 3.5 mm thickness by hot rolling. The chemical compositions of the AZ80 alloy are shown in Table 1.

Table 1 Chemical compositions of AZ80 alloy (mass fraction, %)

Al	Mn	Zn	Ni	Cu	Fe	Be	Mg
8.5	0.32	0.67	0.005	0.05	0.005	0.02	Bal.

Tensile specimens with geometries shown in Fig. 1 were taken along the rolling direction and annealed for 2 h at 430 °C. High temperature tensile tests of elongation-to-failure (EF) and strain-rate-change (SRC) were applied to the annealed specimens on a MTS810 machine equipped with a three-zone resistance furnace. Two thermocouples were contacted to both ends of a specimen to ensure a ±2 °C temperature deviation. EF tests were conducted at strain rates of 10^{-2} and 10^{-3} s^{-1}, and temperatures of 300, 350, 400 and 450 °C, until the specimens fractured. SRC tests were used to evaluate stress exponent at temperatures of 300 350, 400 and 450 °C. In each SRC test, a prestrain was applied to stabilize the testing system and microstructure, followed by nine steps of increasing strain rate from 5×10^{-5} to 2×10^{-2} s^{-1}. In each step, the specimen experienced certain strain until a steady state deformation was reached. True stress and true strain rate were calculated for each step according to load and displacement, and were used to evaluate stress exponent.

Microstructures in the annealed, deformed, and fractured conditions were observed with a JVC TK-350EG optical microscopy (OM) by following standard metallographic procedures and by an etching solution of 5 g picronitric acid, 25 mL ethanoic acid, 100 mL ethyl alcohol, and 10 mL de-ionized water. A scanning electronic microscopy (SEM) of JSM6480LV was applied to the EF specimens to observe fracture patterns.

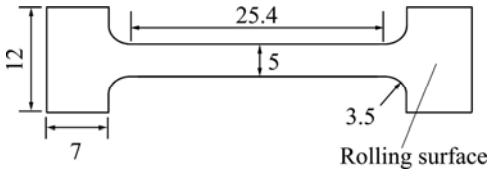

Fig. 1 Specimen geometry for high-temperature tensile test (unit: mm)

3 Results and discussion

3.1 Microstructure

The annealed AZ80 alloy has an equiaxial grain structure with an average grain size of d=16 μm, as shown in Fig. 2 in horizontal rolling orientation.

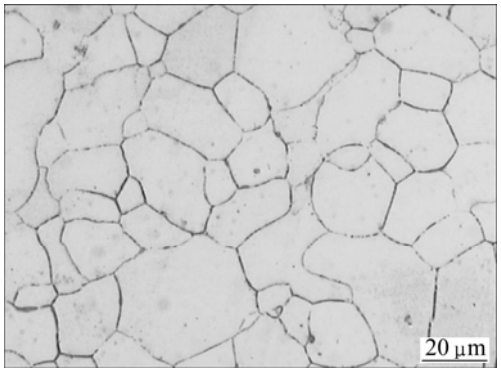

Fig. 2 OM image of annealed AZ80 alloy at 430 °C for 2 h oriented in horizontal rolling direction

Creep mechanisms and models in Mg alloys with low Al contents, such as Mg−0.7Al [12] and AZ31 [6,9], usually assume a stable microstructure because these materials have relatively high stacking fault energy and low possibility of dynamic recrystallization. However, stacking fault energy of Mg alloys decreases significantly with increasing Al content. The stacking fault energy is 78.0 mJ/m^2 for pure Mg, and only 5.8 mJ/m^2 for Mg−9%Al [10]. Therefore, it is necessary to investigate the microstructure stability of AZ80 alloy before any constitutive model can be used.

OM images of AZ80 alloy after the EF test at 400 °C and 10^{-3} s^{-1} in vertical tensile direction are illustrated in Fig. 3. The microstructure in the uniformly deformed gauge, shown in Fig. 3(a), is similar to that in annealed condition, indicating that the microstructure in gauge was stable during deformation. Figure 3(b) shows that coarse grains developed near the fracture, which is similar to the coarse texture reported by SOER et al [13]

in a superplastic Al−Mg−Cu alloy under similar tensile conditions, but was not observed in an extruded AZ31 alloy investigated by authors as described elsewhere [14]. Although the mechanism cannot be conclusively identified from the present results, the coarse grains are presumably attributed to nucleation and propagation of new grains during dynamic recrystallization, which is facilitated by the low stacking fault energy, dislocation density enhancement, and dislocation entanglement induced by the high stress at the fracture. However, it is noted that the coarse grains are accompanied by fine grains, which suggests another possible mechanism of abnormal growth of the original fine grains through second recrystallization. The original fine grains of the investigated alloy were achieved during extrusion and hot rolling process, where new grains nucleated through dynamic recrystallization (first recrystallization) and grain growth may be inhibited by dispersed particles induced by grain-refining alloying additions or crystal textures. During high temperature tensile deformation, these fine grains can grow rapidly through grain boundary migration under the high stress in the necking area. Therefore, the observed coarse grains accompanied by fine grains can result from the second recrystallization process, where the grain-growth inhibiting effect is relative weak under the applied test condition.

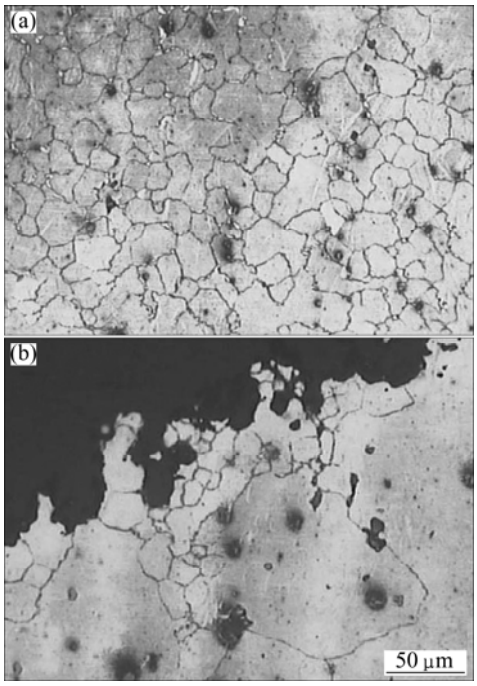

Fig. 3 OM images of AZ80 alloy oriented in vertical tensile direction after EF test at 400 °C and 10^{-3} s^{-1}: (a) Uniformly deformed gauge; (b) Fracture

SEM fracture images of AZ80 alloy after EF test at 10^{-3} s^{-1} are shown in Fig. 4. The river-pattern ductile fracture shows tear ridges, dimples, and cavities. The cavity evolution at 450 °C is more significant than that at 400 °C. Cavity may nucleate at intermetallic particle [15] or grain boundary [16], and grow under either diffusional mechanism for small cavity or plasticity mechanism for large cavities [17]. For the present AZ80 alloy, the particle-stimulated nucleation is not significantly relevant, and the cavities most likely nucleate at grain boundaries and grow with plastic deformation.

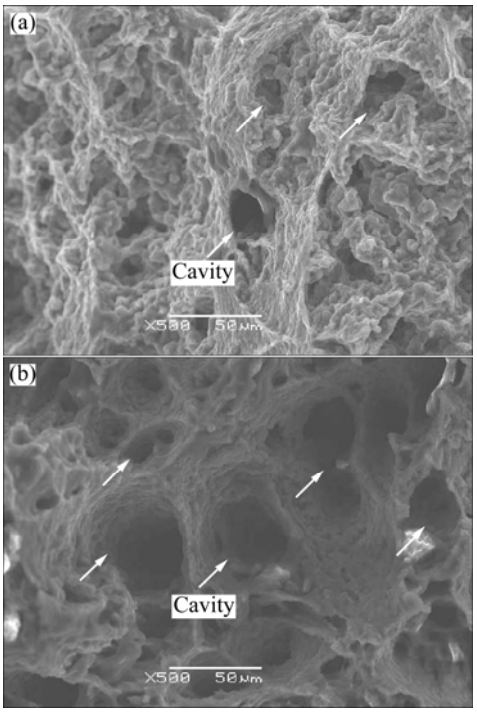

Fig. 4 SEM images of AZ80 alloy after EF test at 10^{-3} s^{-1} and different temperature: (a) 400 °C; (b) 450 °C

3.2 High temperature tensile behavior

True stress and true strain curves in the EF tests at the strain rate of 10^{-2} and 10^{-3} s^{-1} are shown in Fig. 5. The material exhibited evident strengthening followed by quick stress drop at 300 and 350 °C, and less strengthening followed by steady state deformation at 400 and 450 °C. Values of elongation to failure at various temperatures and strain rates are shown in Fig. 6. Elongations at 300 and 350 °C were below 100%, while elongations at 400 and 450 °C were over 100%, and the maximum of 161.15% was achieved at 400 °C and 10^{-2} s^{-1}. The elongation drop from 400 to 450 °C should be attributed to the stronger cavity evolution at 450 °C, as shown in Fig. 4.

Strain-rate-change (SRC) test data are shown in dual logarithmic scale in Fig. 7 as true strain rate versus true stress normalized by elastic modulus of E/MPa= $5.79\times10^4-53.2T$ [10]. The linear relationship at each temperature indicates that a power law is observed, and the slope represents stress exponent (n). Two regions can be specified according to n, one is the low-n region from 5×10^{-5} to 2×10^{-4} s^{-1}, and the other is the

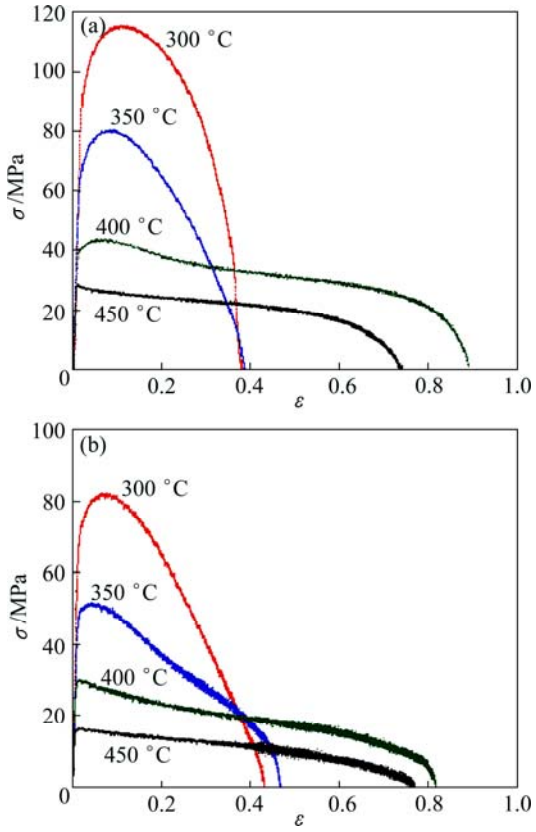

Fig. 5 True stress versus true strain curves of AZ80 alloy in elongation-to-failure tests: (a) $\dot{\varepsilon}=10^{-2}$ s^{-1}; (b) $\dot{\varepsilon}=10^{-3}$ s^{-1}

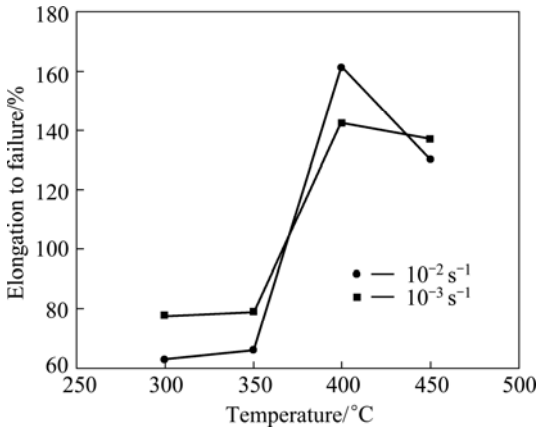

Fig. 6 Elongations under various temperatures and strain rates

high-n region from 5×10^{-4} to 2×10^{-2} s^{-1}. The stress exponents were calculated with linear regression method and summarized in Table 2. The transition from low n to high n with increasing strain rate at each temperature indicates a transition of deformation mechanism.

3.3 Deformation mechanism

High temperature tensile behaviors of crystalline materials are closely related to temperature and strain rate. Strain rate compensated by diffusivity of Al atom in Mg matrix, $\dot{\varepsilon}/D$, was used to construct a $\dot{\varepsilon}/D$—σ/E curve

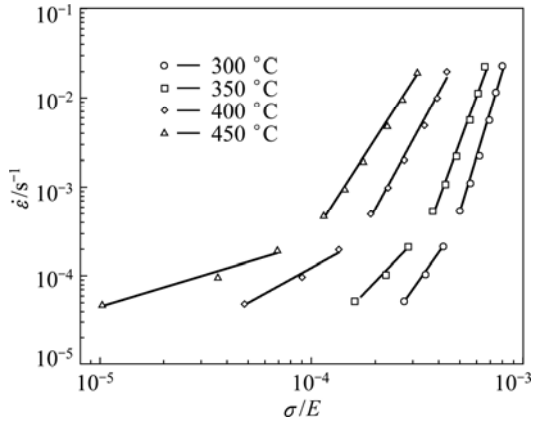

Fig. 7 SRC test data plotted as true strain rate versus modulus-compensated true stress

Table 2 Calculated stress exponent n with linear regression

t/°C	n	
	5×10^{-5} s$^{-1}\leq\dot{\varepsilon}\leq10^{-4}$ s^{-1}	5×10^{-5} s$^{-1}\leq\dot{\varepsilon}\leq2\times10^{-2}$ s^{-1}
300	3.31	8.07
350	2.40	6.52
400	1.31	4.34
450	0.70	3.62

in dual logarithmic scale, as shown in Fig. 8, and $D=D_0\exp(-Q/RT)$, $D_0=1.2\times10^{-3}$ m^{-2}/s, Q=143±10 kJ/mol [18,19]. Similar results can be obtained when the strain rate is compensated by diffusivity of Mg lattice diffusion with $D_0=1.0\times10^{-4}$ m^{-2}/s and Q=135 kJ/mol [20]. Three regions were specified according to n value: low-n region where n=1.79, 1.78×10^{9} m$^{-2}\leq\dot{\varepsilon}/D\leq4.14\times10^{10}$ m^{-2}; intermediate-n region where n=4.29, 5.01×10^{10} m$^{-2}\leq\dot{\varepsilon}/D\leq4.82\times10^{12}$ m^{-2}; high-n region where n=9.54 and 9.62×10^{12} m$^{-2}\leq\dot{\varepsilon}/D\leq2.07\times10^{14}$ m^{-2}. The high-n region is usually considered as a transition to power law breakdown at low temperature and high strain rate.

The investigated AZ80 alloy exhibits elongations of over 100% at temperatures of 400 and 450 °C and initial

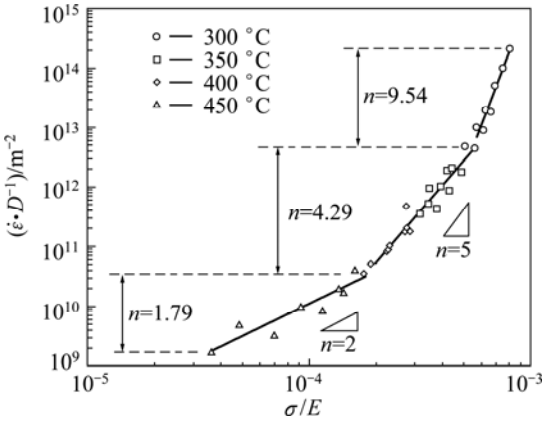

Fig. 8 SRC test data plotted as diffusivity-compensated true strain rate versus modulus-compensated true stress

strain rates of 10^{-2} and 10^{-3} s^{-1}, which give approximately 1.04×10^{11} $m^{-2} \leq \dot{\varepsilon}/D \leq 1.789\times10^{11}$ m^{-2}, and fall into the intermediate region of n=4.29. The deformation activation energy, Q, for this region is calculated using the follow equation [4]:

$$Q = \left(\frac{nR\partial \ln\sigma}{\partial(1/T)}\right)_{\dot{\varepsilon}} \quad (3)$$

where n=4.29, the flow stress of σ is taken at true strain of 0.2 at each temperature in Fig. 5 to build the relationship in Fig. 9. The calculated activation energy is 149.60 kJ/mol, which approximates both that of 135 kJ/mol for Mg lattice diffusion and that of 143±10 kJ/mol for Al diffusion in Mg. According to the calculated stress exponent and activation energy, dislocation climb creep (DCC) seems to be responsible for the enhanced ductilities, and deformation is rate controlled by dislocation climb through lattice diffusion. However, the investigated alloy has relatively fine grain structure and high Al content, so grain boundary sliding (GBS) and solute drag creep (SDC) must be discussed as the potential mechanisms.

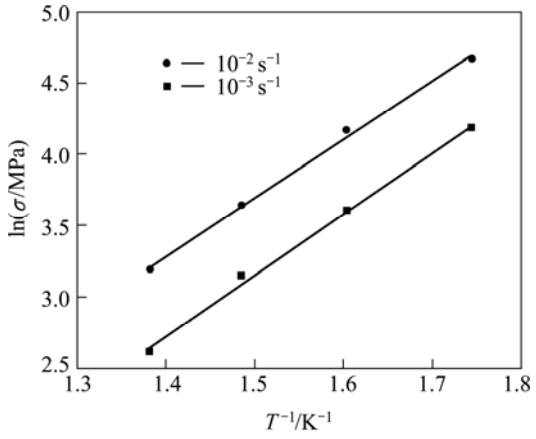

Fig. 9 Calculation of creep activation energy

SDC operates by retarding dislocation glide through elastic interaction between solute atoms and dislocations in a coarse and stable microstructure. In the present AZ80 alloy, Al atoms either exist in $Mg_{17}Al_{12}$ precipitates or dissolve in Mg matrix as solute atoms. Based on the Mg−Al phase diagram, melting temperature of $Mg_{17}Al_{12}$ in AZ80 alloy is about 350 °C, which indicates that most $Mg_{17}Al_{12}$ precipitates dissolve at 400 and 450 °C, and Al solute atoms may interact with dislocations to assist SDC mechanism. However, based on the microstructure study, the investigated alloy has a stable fine-grained structure (16 μm) in the gauge where most of the elongation occurs. This fine-grained structure usually does not facilitate significant SDC operation, but facilitates GBS at high temperature and low strain rate.

GBS operates by grain boundary diffusion or lattice diffusion and requires a fine and stable microstructure. In the low stress exponent region of n=1.79 (high temperature and low strain rate), grain boundary sliding and grain rotation during GBS can induce stress concentration when diffusion is not capable of coordinating deformation. Dislocations are emitted from grain boundary to release the stress concentration. These emitted dislocations and original intragranular dislocations slip and climb to grain boundaries to assist GBS [21]. In the intermediate region of n=4.29 (lower temperature and higher strain rate) where high elongations is achieved, GBS alone is not capable of coordinating deformation at lower diffusivity and higher strain rate, while dislocations are more active in the thermally activated prismatic and pyramidal slip systems. Therefore, DCC becomes more significant and the high ductilities should be attributed to a competitive deformation mechanism of GBS and DCC.

$$\frac{\dot{\varepsilon}}{D} = 1.60\times10^{17}\left(\frac{\sigma}{E}\right)^{1.79} + 3.91\times10^{26}\left(\frac{\sigma}{E}\right)^{4.29} \quad (4)$$

Consistent with the two-mechanism interpretation, a phenomenological equation (Eq. (4)) using the stress exponent for GBS (n=1.79) and the stress exponent for DCC (n=4.29) is established to formulate a constitutive model [22]. The model is successfully fit to the data in Fig. 8, as shown in Fig. 10, and with this model, plane strain deformation of AZ80 sheet can be evaluated with specific diffusivity, elastic modulus, and stress exponent.

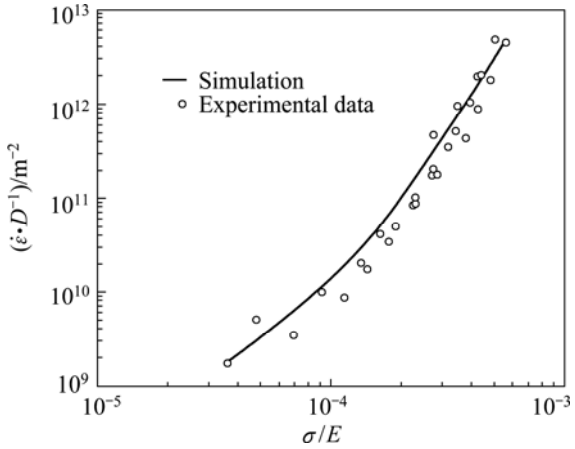

Fig. 10 Simulation with two-mechanism phenomenological equation

4 Conclusions

1) AZ80 alloy with an initial average grain size of 16 μm exhibits enhanced elongation-to-failure ductilities of higher than 100% during steady-state deformation at 400 and 450 °C under strain rates of 10^{-2} and 10^{-3} s^{-1}, while elongations at 300 and 350 °C are less than 100% without steady-state deformation.

2) Original fine grain structure is stable in the uniformly deformed gauge during the tensile deformation achieving the enhanced ductilities. Cavities develop significantly in fractures with increasing temperature from 400 to 450 °C when deformed at 10^{-3} s^{-1}, and tensile elongation drops correspondingly.

3) The enhanced ductilities of over 100% are featured by a stress exponent of 4.29 and an activation energy of 149.60 kJ/mol, and are rate controlled by a competitive mechanism of grain boundary sliding and dislocation climb creep, which can be simulated by a two-mechanism model using regressed stress exponents.

References

[1] WATARAI H. Trend of research and development for magnesium alloys—Reducing the weight of structural materials in motor vehicles [J]. Science and Technology Trends, 2006, 18: 84−97.

[2] YI Li, CHENG Pei-yuan, LIN Hua. Current application of magnesium alloy in automotive industry and 3C product fields [J]. Jiangxi Nonferrous Metals, 2007, 21(2): 30−33. (in Chinese)

[3] MUKHERJEE A K, BIRD J E, DORN J E. Experimental correlations for high-temperature creep [J]. Transactions of the ASM, 1969, 62: 155−179.

[4] WEI Y H, WANG Q D, ZHU Y P, ZHOU H T, DING W J, CHINO Y, MABUCHI M. Superplasticity and grain boundary sliding in rolled AZ91 magnesium alloy at high strain rates [J]. Materials Science and Engineering A, 2003, 360(1−2): 107−115.

[5] FIGUEIREDO R B, LANGDON T G. Principles of grain refinement and superplastic flow in magnesium alloys processed by ECAP [J]. Materials Science and Engineering A, 2009, 501(1−2): 105−114.

[6] FIGUEIREDO R B, LANDON T G. Developing superplasticity in a magnesium AZ31 alloy by ECAP [J]. Journal of Materials Science, 2008, 43(23−24): 7366−7371.

[7] BOILEAU J M, FRIEDMAN P A, HOUSTON D Q, LUCKEY S G. Superplastic response of continuously cast AZ31B magnesium sheet alloys [J]. Journal of Materials Engineering and Performance, 2010, 19(4): 467−480.

[8] GARCÍA-BERNAL M A, HERNANDEZ-SILVA D, SAUCE-RANGEL V. Superplastic behavior of coarse-grained Al−Mg−Zn alloys [J]. Journal of Materials Science, 2007, 42(11): 3958−3963.

[9] VALLE J A D, PÉREZ-PRADO M T, RUANO O A. Deformation mechanisms responsible for the high ductility in a Mg AZ31 alloy analyzed by electron backscattered diffraction [J]. Materials Science and Engineering A, 2005, 36(6): 1427−1438.

[10] SOMEKAWA H, HIRAI K, WATANABE H, TAKIGAWA Y, HIGASHI K. Dislocation creep behavior in Mg−Al−Zn alloys [J]. Materials Science and Engineering A, 2005, 407(1−2): 53−61.

[11] WATANABE H, TSUTSUI H, MUKAI T, KOHZU M, TANABE S, HIGASHI K. Deformation mechanism in a coarse-grained Mg−Al−Zn alloy at elevated temperatures [J]. International Journal of Plasticity, 2001, 17(3): 387−397.

[12] KOTTADA R S, CHOKSHI A H. Grain boundary sliding during diffusion and dislocation creep in a Mg−0.7 Pct Al alloy [J]. Metallurgical and Materials Transactions A, 2007, 38(8): 1743−1749.

[13] SOERA W A, CHEZANA A R, HOSSON J T M D. Deformation and reconstruction mechanisms in coarse-grained superplastic Al–Mg alloys [J]. Acta Materialia, 2006, 54(14): 3827−3833.

[14] QIAO Jun, WANG Yu, SHI Guo-dong. High temperature tensile behaviors of extruded and rolled AZ31 Mg alloy [J]. Transactions of Nonferrous Metals Society of China, 2010, 20(S2): s540−s544.

[15] CHANG J K, TALEFF E M, KRAJEWSKI P E. Effects of microstructure on cavitation during hot deformation of a fine-grained aluminum-magnesium alloy as revealed through three-dimensional characterization [J]. Metallurgical and Materials Transactions A, 2009, 40(13): 3128−3135.

[16] WEN L Z, PING P W, JIE L P, PING L L. Cavity evolution behavior of twin-roll-cast AZ31 alloy sheet during hot deformation [J]. The Chinese Journal of Nonferrous Metals, 2009, 19(5): 785−792. (in Chinese)

[17] TAKIGAWA Y, AGUIRRE J V, TALEFF E M, HIGASHI K. Cavitation during grain-boundary-sliding deformation in an AZ61 magnesium alloy [J]. Materials Science and Engineering A, 2008, 497(1−2): 139−146.

[18] MCNELLEY T R, MICHEL D J, SALAMA A. The Mg-concentration dependence of the strength of Al−Mg alloys during glide-controlled deformation [J]. Scripta Metallurgica, 1989, 23(10): 1657−1662.

[19] VAGARALI S S, LANGDON T G. Deformation mechanisms in h.c.p. metals at elevated temperatures-II. Creep behavior of a Mg−0.8%Al solid solution alloy [J]. Acta Metallurgica, 1982, 30(6): 1157−1170.

[20] FROST H J, ASHBY M F. Deformation mechanism maps: the plasticity and creep of metals and ceramics [M]. Oxford, UK: Pergamon Press, 1982: 43−44.

[21] ZHANG S C, ZONG Q, HU Y S, CHENG X R. Creep property and mechanism of AZ31 magnesium alloy under high temperature and low stress [J]. Journal of Mechanical Engineering, 2009, 45(3): 291−295.

[22] VERMA R, HECTOR L G, KRAJEWSKI P E, TALEFF E M. The finite element simulation of high-temperature magnesium AZ31 sheet forming [J]. Journal of the Minerals Metals and Materials Society, 2009, 61(8): 29−37.

AZ80 镁合金的高温拉伸变形行为

乔 军，边福勃，何 敏，王 瑜

辽宁科技大学 材料与冶金学院，鞍山 114051

摘 要：采用拉伸至断裂实验，在温度为 300、350、400 和 450 °C，应变率分别为 10^{-2} 和 10^{-3} s^{-1} 条件下，研究 AZ80 镁合金的拉伸行为。并采用变化应变率拉伸实验在 5×10^{-5} 至 2×10^{-2} s^{-1} 的应变率范围内进行变形机制研究。结果表明：该材料在 400 和 450 °C 下具有超过 100%的高伸长率，其应力指数为 4.29，变形激活能为 149.60 kJ/mol。初始细晶粒在均匀变形区的高温变形中较为稳定，其变形机制为晶界滑移和位错攀移蠕变的竞争机制。基于该机制所建立的数学模型的模拟结果与实验数据吻合。

关键词：AZ80 镁合金；拉伸行为；超塑性；蠕变；应力指数

(Edited by Chao WANG)